IPPP/01/53
DCPT/01/106
20 February 2002

Prospects for New Physics observations in diffractive processes at the LHC and Tevatron

V.A. Khoze[a], A.D. Martin[a], and M.G. Ryskin[a,b]

[a] Department of Physics and Institute for Particle Physics Phenomenology, University of Durham, Durham, DH1 3LE
[b] Petersburg Nuclear Physics Institute, Gatchina, St. Petersburg, 188300, Russia

Abstract

We study the double-diffractive production of various heavy systems (e.g. Higgs, dijet, $t\bar{t}$ and SUSY particles) at LHC and Tevatron collider energies. In each case we compute the probability that the rapidity gaps, which occur on either side of the produced system, survive the effects of soft rescattering and QCD bremsstrahlung effects. We calculate both the luminosity for different production mechanisms, and a wide variety of subprocess cross sections. The results allow numerical predictions to be readily made for the cross sections of all these processes at the LHC and the Tevatron collider. For example, we predict that the cross section for the *exclusive* double-diffractive production of a 120 GeV Higgs boson at the LHC is about 3 fb, and that the QCD background in the $b\bar{b}$ decay mode is about 4 times smaller than the Higgs signal if the experimental missing-mass resolution is 1 GeV. For completeness we also discuss production via $\gamma\gamma$ or WW fusion.

1 Introduction

Double-diffractive processes of the type

$$pp \;\rightarrow\; X + M + Y, \tag{1}$$

can significantly extend the physics programme at high energy proton colliders. Here M represents a system of invariant mass M, and the + signs denote the presence of rapidity gaps which separate the system M from the products X and Y of proton diffractive dissociation. Such processes allow both novel studies of QCD at very high energies and searches for New Physics. From a theoretical point of view, hadronic processes containing rapidity gaps play a crucial role in determining the asymptotic behaviour of the cross section at high energies. From an experimental viewpoint, the presence of rapidity gaps provides a clean environment for the identification of a signal. In such events we produce a colour-singlet state M which is practically free from soft secondary particles.

Double-diffractive *exclusive* processes of the type

$$pp \;\rightarrow\; p \;+\; M \;+\; p, \tag{2}$$

where the protons remain intact, are even better. They allow the reconstruction of the "missing" mass M with good resolution, and so provide an ideal way to search for new resonances and threshold behaviour phenomena. Moreover, in exclusive processes with forward protons, as shown in Fig. 1(a), the incoming gg state satisfies special selection rules, namely it has $J_z = 0$, and positive C and P parity. Hence only a subset of resonant states M can be produced, in particular 0^{++} (but not, for example, 1^{++}). Furthermore, the selection rules control the threshold behaviour of the production of a pair of heavy particles. For example, the Born cross section for the production of a fermion-antifermion pair is proportional to β^3, where β is the fermion velocity, while for scalar particles the threshold behaviour is just β. Thus, for instance, in this way we can distinguish between scalar quark, $\tilde{q}$, and gluino, $\tilde{g}$, pair production. Also, the selection rules are of crucial importance in suppressing the $b\bar{b}$ QCD background when searching for the $H \rightarrow b\bar{b}$ signal [1, 2].

We may write the cross sections for processes (1) and (2) in the factorized form

$$\sigma \;=\; \mathcal{L}(M^2, y)\, \hat{\sigma}(M^2), \tag{3}$$

where $\hat{\sigma}$ is the cross section for the hard subprocess which produces the system of mass M, and $\mathcal{L}$ is the effective luminosity for production at rapidity y. The luminosity $\mathcal{L}$ may refer to any colourless t-channel states which transfer energy across the rapidity gaps without radiating secondary particles. For example, the colourless exchange may be a two-gluon 'hard Pomeron' state, or a phenomenological 'soft' Pomeron, or even a γ or W boson.

The aim of the present paper is to provide a comprehensive way to estimate the numerical size of the cross sections for all these double-diffractive mechanisms for producing a wide range

of heavy systems M (for example, Higgs, dijet, $t\bar{t}$ and SUSY particles). First, in Section 2 we determine the luminosity for the different double-diffractive production mechanisms. We present plots which readily give the luminosity as a function of the mass M and rapidity y of the heavy system, for $pp(\bar{p}p)$ collider energies $\sqrt{s} = 2, 8$ and 14 TeV. Then in Section 3 we give the formulae for, and numerical estimates of, the hard subprocess cross section $\hat{\sigma}$ for the different heavy systems M. Armed with this numerical information of $\mathcal{L}$ and $\hat{\sigma}$, we can immediately estimate the observable cross sections σ of a wide variety of different double-diffractive processes at the LHC and the Tevatron, see (3).

We consider the following double-diffractive mechanisms. Production of the heavy system

(a) via the exclusive process $pp \to p + M + p$, shown in (2),

(b) via the inclusive process $pp \to X + M + Y$, shown in (1),

(c) via the inelastic collision of two Pomerons.

The three different mechanisms are shown in Fig. 1. Since we are considering the production of a massive system M at high collider energy, the luminosity of the first two mechanisms may be calculated from perturbative QCD, using the known parton distributions of the proton. Although the cross section $\hat{\sigma}$ for the hard subprocess is factored off, recall that there may exist specific selection rules for the different configurations. In particular in the case of exclusive production only the projection with $J_z = 0$ and $P = +1$ contributes to $\hat{\sigma}$.

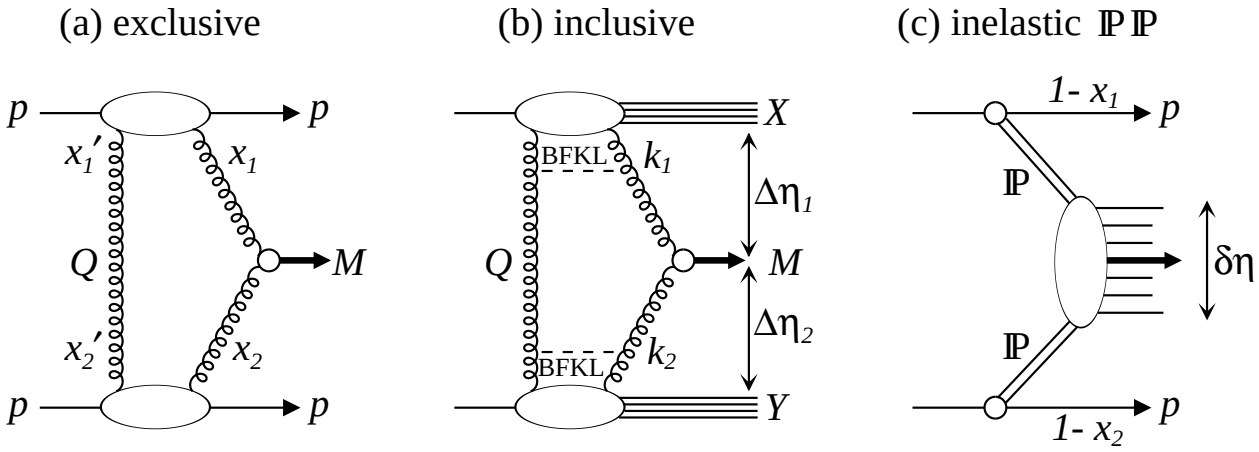

Figure 1: Different mechanisms for the double-diffractive production of a system of mass M in high energy proton-proton collisions.

We need to be careful in interpreting the cross section $\hat{\sigma}$ for the subprocess producing the massive system, $gg \to M$. It corresponds to *colour singlet* production. That is the subprocess

amplitude is averaged over the colour indices of the incoming gluons

$$\mathcal{M} \;=\; \frac{1}{N_C^2-1}\sum_{a,b}\mathcal{M}_{ab}\,\delta_{ab}, \tag{4}$$

where $N_C = 3$ and $\mathcal{M}_{ab}$ is the amplitude for the fusion subprocess $g^a g^b \to M$. All other colour factors are included in the luminosity. Moreover, in the case of exclusive double-diffractive production, the *amplitudes* (rather than the cross sections) are averaged over the two *transverse* polarisations of the incoming gluons

$$\mathcal{M} \;=\; \frac{1}{2}\sum_{\varepsilon_1,\varepsilon_2}\mathcal{M}^{\varepsilon_1,\varepsilon_2}\,\delta_{\varepsilon_1\varepsilon_2}. \tag{5}$$

As a consequence, at leading order, we have only $J_z = 0$ production. On the contrary, for inclusive production, the subprocess *cross section* is averaged over *all* polarisation states of the incoming gluons, as usual. Finally note that for production via soft Pomeron-Pomeron fusion, the cross section $\hat{\sigma}$ includes the convolution with the parton distributions of the Pomeron.

2 Luminosities for double-diffractive processes

In this section we collect together the formulae necessary to compute the luminosity functions for the processes shown in Fig. 1. We write the effective[1] luminosities, for producing a system of mass M and rapidity y, in the form

$$M^2\,\frac{\partial\mathcal{L}^{(i)}}{\partial y\,\partial M^2} \;=\; \hat{S}^{2(i)}\,L^{(i)}, \tag{6}$$

with $i = a, b, c$ corresponding to the processes shown in Fig. 1. Here we have integrated over the transverse momenta of the outgoing protons or outgoing proton dissociated systems, according to whether we are considering exclusive or inclusive double diffractive production. An important ingredient in the calculation of the luminosity is the inclusion of the survival probability of the rapidity gaps to, first, soft rescattering of the interacting protons and, second, to QCD radiation. The latter, which results in a Sudakov-like suppression, is included in the expressions for $L^{(i)}$ below. The soft rescattering effects are symbolically denoted by a factor $\hat{S}^2$ in (6). In practice, we calculate the effects using a two-channel eikonal. As a consequence (6) does not have a factorized form, and $\hat{S}^2$ should be viewed as the soft survival probability appropriately averaged over the channels [3, 4]. The value of the survival factor $\hat{S}^2$ depends on the particular double-diffractive production mechanism, and may be a function of y and M^2.

[1]The Pomeron should be regarded as including all multi-Pomeron effects.

2.1 Exclusive double-diffractive production

For the exclusive process shown in Fig. 1(a) we have, to single log accuracy, [5]

$$L^{\rm excl} \;=\; \left(\frac{\pi}{(N_C^2-1)b}\int \frac{dQ_t^2}{Q_t^4}\, f_g(x_1,x_1',Q_t^2,\mu^2)\, f_g(x_2,x_2',Q_t^2,\mu^2)\right)^2, \tag{7}$$

where b is the t-slope corresponding to the momentum transfer distributions of the colliding protons

$$\frac{d^2\sigma}{dt_1 dt_2} \;\propto\; e^{b(t_1+t_2)}, \tag{8}$$

where we take[2] $b = 4$ GeV^{-2}. The quantities $f_g(x,x',Q_t^2,\mu^2)$ are the generalised (skewed) unintegrated gluon densities of the protons. The skewed effect arises because the screening gluon (Q_t) carries a much smaller momentum fraction $x' \ll x$. For small $|x-x'|$ the skewed unintegrated density can be calculated from the conventional integrated gluon $g(x,Q_t^2)$ [7]. However the full prescription is rather complicated. For this reason it is often convenient to use the simplified form [5]

$$f_g(x,x',Q_t^2,\mu^2) \;=\; R_g\,\frac{\partial}{\partial \ln Q_t^2}\left[\sqrt{T(Q_t,\mu)}\,xg(x,Q_t^2)\right], \tag{9}$$

which holds to 10–20% accuracy. The factor R_g accounts for the single log Q^2 skewed effect [8]. It is found to be about 1.2 at the LHC energy, and 1.4 at the Tevatron energy. The Sudakov factor $T(Q_t,\mu)$ is the survival probability that a gluon with transverse momentum Q_t remains untouched in the evolution up to the hard scale $\mu = M/2$

$$T(Q_t,\mu) \;=\; \exp\left(-\int_{Q_t^2}^{\mu^2}\frac{\alpha_S(k_t^2)}{2\pi}\,\frac{dk_t^2}{k_t^2}\int_0^{1-\Delta}\left[zP_{gg}(z)\;+\;\sum_q P_{qg}(z)\right]dz\right), \tag{10}$$

with $\Delta = k_t/(\mu+k_t)$. The square root arises in (9) because the survival probability is only relevant to the hard gluon. It is the presence of this Sudakov factor which makes the integration in (7) infrared stable, and perturbative QCD applicable.

The luminosities $M^2 d\mathcal{L}/dydM^2$ calculated from (7) and (6) for the exclusive double-diffractive production of a system of invariant mass M and rapidity y are shown by the solid continuous curves, denoted *excl*, in Figs. 2, 3 and 4. Fig. 2 shows the dependence of the luminosity on M at $y = 0$, and Figs. 3 and 4 show the dependence on y for produced masses of $M = 120$ and $M = 500$ GeV respectively, at various pp (or $p\bar{p}$) collider energies. We use the MRST99

[2] If we were to adopt a Regge interpretation, then the 'Pomeron' would be represented in (7) by an unintegrated gluon distribution f_g which, for a large hard scale μ, is described by DGLAP evolution. As a consequence of the strong k_t ordering, the position of the gluons in impact parameter space is frozen, and hence there is no shrinkage of the diffraction cone. This would mean that the corresponding Pomeron trajectory would have zero slope, $\alpha' = 0$. Therefore we choose a constant t-slope, b, which characterises the t dependence of the Pomeron-proton vertex. The value $b = 4$ GeV^{-2} is taken from the fit to the soft hadronic data of Ref. [3]. This value is consistent with that observed in J/ψ diffractive production at HERA [6].

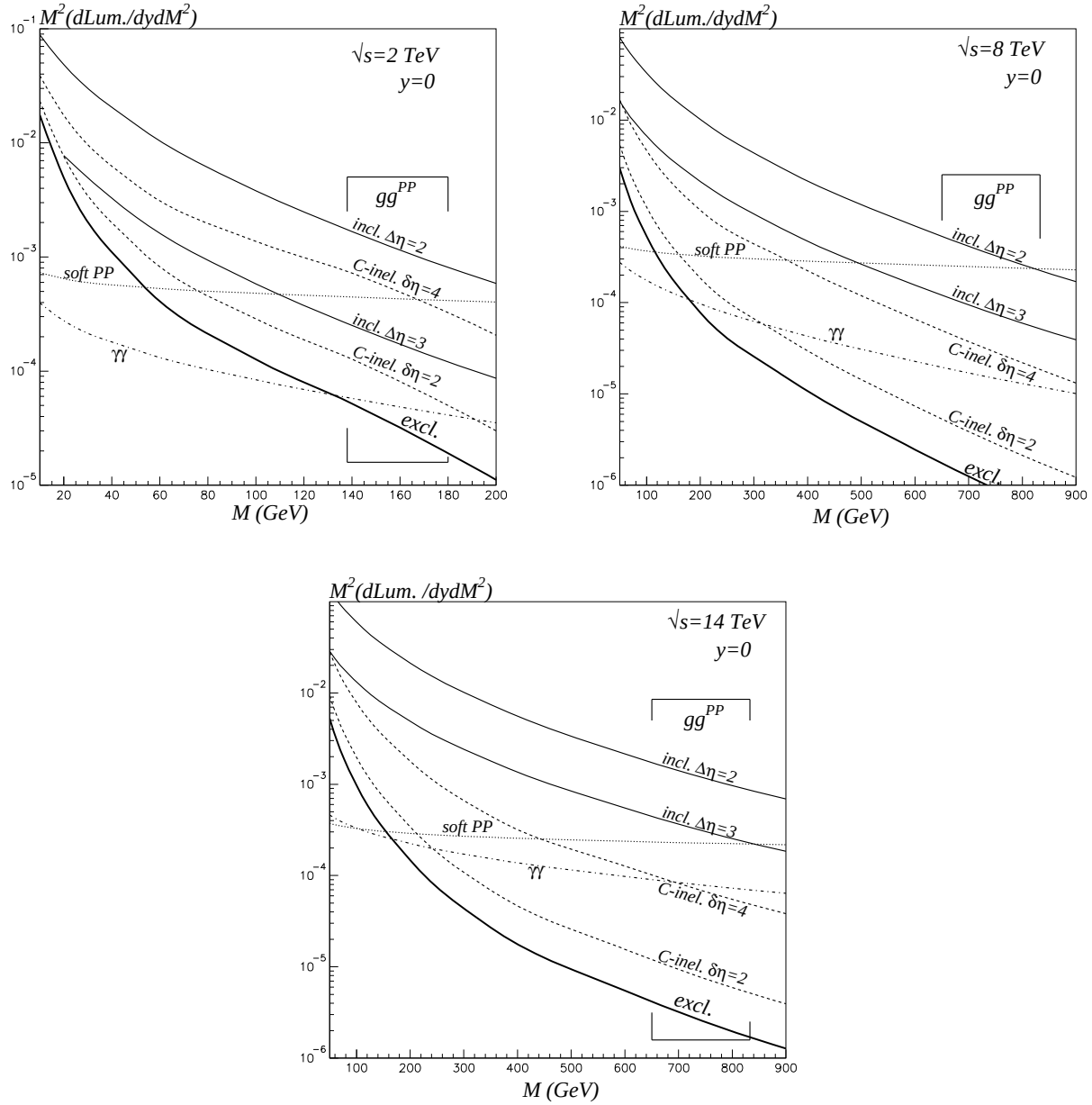

Figure 2: The luminosity $M^2\partial\mathcal{L}/\partial y\partial M^2$ versus M, for the double-diffractive production of a heavy system of mass M with rapidity $y = 0$. The three plots are for pp (or $p\bar{p}$) collider energies of $\sqrt{s} = 2, 8$ and 14 TeV. Various production mechanisms are studied: the curves marked *excl.*, *incl.*, *C-inel* and *soft I\!P I\!P* correspond, respectively, to production by the exclusive process $pp \to p + M + p$ of Section 2.1, to production by the inclusive process $pp \to X + M + Y$ of Section 2.2, and to production by the processes shown in Figs. 6(a) and 6(b) as described in Section 2.3. The $\gamma\gamma$ luminosity is obtained as described in Section 2.4.

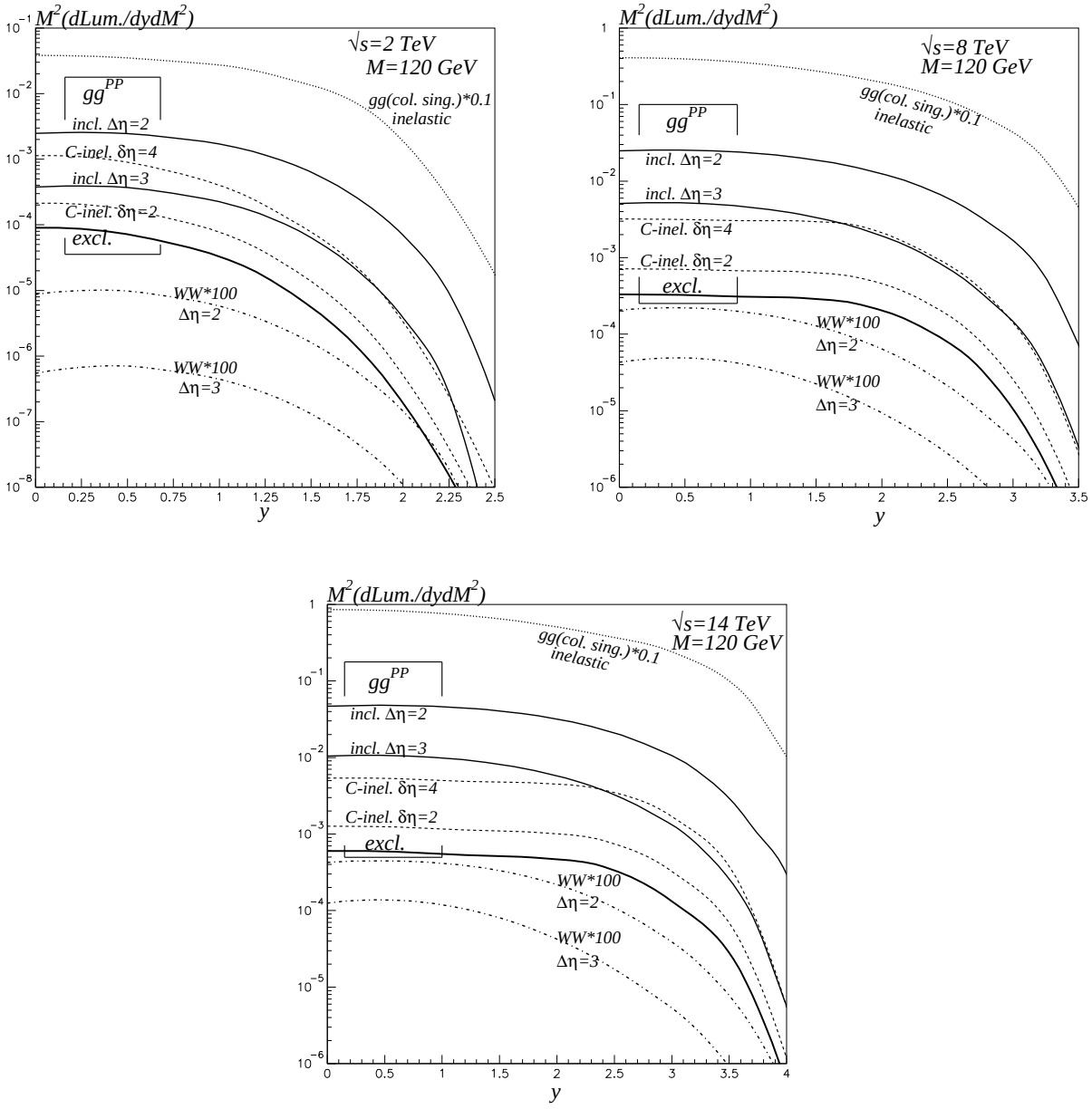

Figure 3: The luminosity $M^2\partial\mathcal{L}/\partial y\partial M^2$ versus y for the double-diffractive production by various mechanisms of a heavy system of mass $M = 120$ GeV at $\sqrt{s} = 2, 8$ and 14 TeV. The notation for the curves is as in Figs. 2 and 6. The upper curve in each plot shows the inelastic luminosity ($\Delta\eta = 0$) assuming that the fusing gg pair are in a colour singlet state.

partons [9] to calculate the unintegrated gluon distributions (9), and we calculate the 'soft' survival factor $\hat{S}^2$ using the formalism of Ref. [3]. We find $\hat{S}^2 = 0.045$, 0.026 and 0.020 for collider energies $\sqrt{s} = 2, 8$ and 14 TeV respectively.

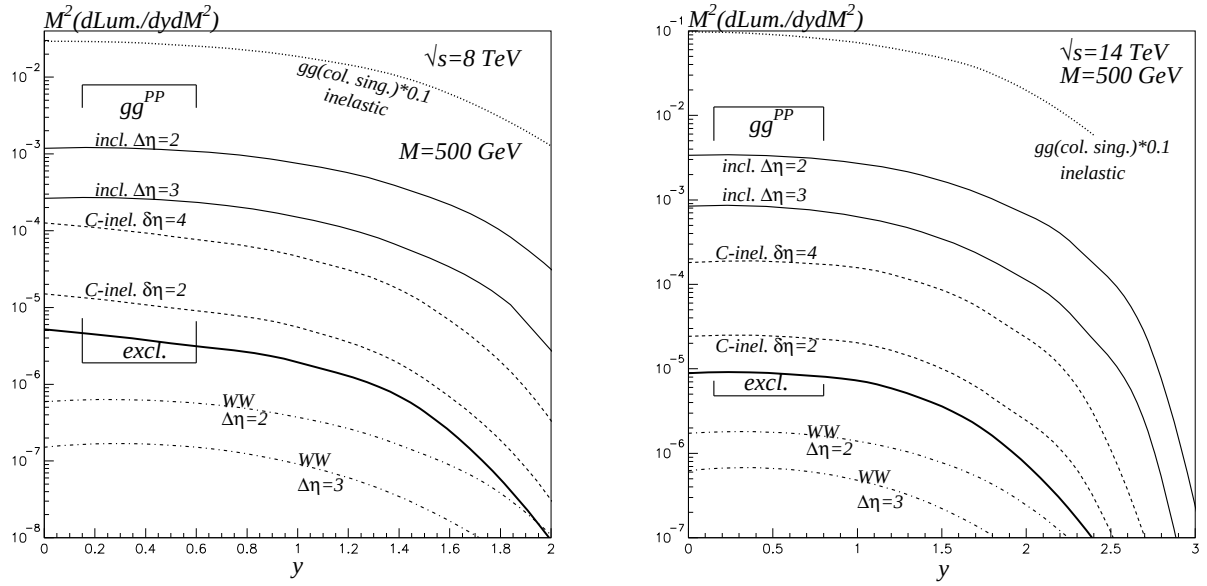

Figure 4: As for Figure 3, but for the production of a system of mass $M = 500$ GeV at pp collider energies of $\sqrt{s} = 8$ and 14 TeV.

The luminosity is presented as the number of effective gluon-gluon collisions per pp interaction. In Figs. 2 and 3 we denote it as gg^{PP} to indicate that the hard gluons, which interact to form the system M, originate within overall colourless (hard Pomeron) t-channel exchanges, see Fig. 1(a). This is precisely the quantity which must be multiplied by the cross section $\hat{\sigma}$ of the $J_z = 0$, colour-singlet hard subprocess $gg \to M$, to form the double-diffractive cross section σ of (3).

As can be seen from Fig. 2 the luminosity decreases with increasing M, but grows with the collider energy $\sqrt{s}$. The reason is that there is an increasing number of gluons as x becomes smaller, and because for larger M the double-logarithmic Sudakov suppression (10) is stronger due to the higher scale $\mu = M/2$.

2.2 Inclusive double-diffractive production

Exclusive production has by far the cleanest signal. Unfortunately, the luminosity, and hence the predicted event rate, are small. For this reason we consider *inclusive* double diffractive production, process (1), with less restrictive kinematics due to the dissociation of the incoming protons, see Fig. 1(b). The cross section can be expressed as exclusive production at the parton-parton level

$$a_1 a_2 \;\to\; a_1 \;+\; M \;+\; a_2, \tag{11}$$

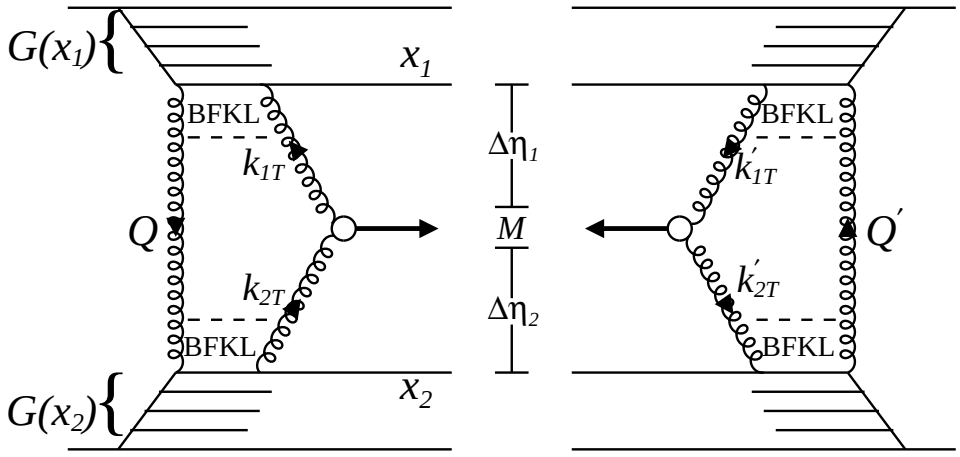

Figure 5: The amplitude of Fig. 1(b) multiplied by its complex conjugate, which gives the cross section for the inclusive double-diffractive production of a system M. The effective parton densities, $G(x_i)$ of (19), are to be evaluated at scales k_{it}^2.

convoluted with the probabilities to find partons a_1, a_2 in the incoming protons. The process is shown in Fig. 5, where the probabilities are denoted by the effective parton densities $G(x_i)$. At the parton-parton level, (11), the unintegrated gluon distributions in partons a_1, a_2 may be calculated perturbatively in terms of the non-forward BFKL amplitudes A_1, A_2. This means that we must replace the densities f_g in (7) by $A_i\sqrt{T_i}$, where $T_i \equiv T(k_{it}, \mu)$ is given by (10). The non-forward BFKL amplitudes A_i are of the form [11]

$$A_i \;=\; \exp(-n_i/2)\,\Phi(Y_i), \tag{12}$$

where n_i is the mean number of gluons emitted, with transverse momenta in the range (Q_t, k_{it}) and rapidities in the interval $\Delta\eta_i$

$$n_i \;=\; \frac{3\alpha_S}{\pi}\,\Delta\eta_i\,\ln\left(\frac{k_{it}^2}{Q_t^2}\right). \tag{13}$$

The remaining factor $\Phi(Y_i)$ accounts for the usual BFKL (single) logarithms. For rapidity gaps $\Delta\eta_i < 4$ we have

$$Y_i \;\equiv\; \frac{3\alpha_S}{2\pi}\,\Delta\eta_i \;\lesssim\; 0.4, \tag{14}$$

and, for $Q_t^2 \ll k_{it}^2$, it is sufficient to retain only the $O(Y_i)$ term, which gives [11]

$$\Phi(Y_i) \;\simeq\; 1 \,+\, Y_i\,\frac{Q_t^2}{k_{it}^2} \;\simeq\; 1.1 \,\pm\, 0.1. \tag{15}$$

We use this value in our numerical predictions. Note that the BFKL amplitudes, which describe elastic parton-parton scattering, already contain the double-logarithmic Sudakov suppression

which reflects the absence of secondary gluon emission with transverse momenta p_t up to the momentum transfer k_{ti}. The remainder of the hard suppression factor, which accounts for the absence of emission in the interval (k_{ti}, μ), has been incorporated separately in terms of the survival factors T_i.

The dominant (leading log) contribution to the inclusive amplitude of Fig. 1(b) comes from the asymmetric configuration $Q_t^2 \ll k_{it}^2$. Thus the transverse momenta of the two hard active gluons can no longer be approximated by $k_{it} \approx Q_t$, as they were in the exclusive case in (7) [5]. As a consequence each hard gluon propagator, together with its polarization factor, can no longer be written as Q_t/Q_t^2, but must remain k_{it}/k_{it}^2. Therefore, the factor $1/Q_t^4$ in the amplitude in (7) now becomes $1/(Q_t^2 k_{1t} k_{2t})$. Moreover, in the limit $Q_t^2 \ll k_{it}^2$ we have $k_{it} \simeq k'_{it}$. Thus, instead of the factor $1/b$, which came from the t_i integral limited by the proton form factor as in (7) and (8), we now obtain the logarithmic dk_{it}^2/k_{it}^2 integrals. Here we have used

$$t_i \;=\; (Q - k_i)^2 \;\simeq\; -k_{it}^2 \;\simeq\; -k_{it}'^2. \tag{16}$$

Thus, to compute Fig. 5 we must evaluate

$$\mathcal{I} \;=\; \int \frac{dQ_t^2}{Q_t^2}\,\frac{dQ_t'^2}{Q_t'^2}\,\frac{dk_{1t}^2}{k_{1t}^2}\,\frac{dk_{2t}^2}{k_{2t}^2}\,(A_1 A_2 A_1' A_2')\,\sqrt{T_1 T_1' T_2 T_2'}. \tag{17}$$

In this way, we find the luminosity, (6), for the inclusive process of Fig. 1(b) and Fig. 5, in which the initial protons dissociate and the system M is produced with rapidity gaps $\Delta\eta_1$ and $\Delta\eta_2$ on either side, is, to leading log accuracy, expressed in the form [10]

$$L^{\rm incl} \;=\; \int_{x_1^{\rm min}}^1 G(x_1)\,\frac{dx_1}{x_1}\int_{x_2^{\rm min}}^1 G(x_2)\,\frac{dx_2}{x_2}\,\frac{\alpha_S^4}{\pi^2}\left(\frac{N_C^2}{N_C^2-1}\right)^2\mathcal{I}, \tag{18}$$

with $N_C = 3$. The primed quantities arise because the luminosity is obtained by multiplying the inclusive amplitude by its complex conjugate, as in Fig. 5. The effective parton densities,

$$G(x_i) \;=\; x_i g(x_i, k_{it}^2) \;+\; \frac{16}{81}\sum_q x_i\left(q(x_i, k_{it}^2) \;+\; \bar{q}(x_i, k_{it}^2)\right), \tag{19}$$

are integrated from

$$x_i^{\rm min} \;=\; \frac{M}{\sqrt{s}}\,e^y \;+\; \frac{k_{it}}{\sqrt{s}}\,e^{(y+\Delta\eta_i)} \tag{20}$$

up to 1. These limits ensure that no recoil jets in the dissociated states X and Y lie within the rapidity gap intervals $\Delta\eta_1$ and $\Delta\eta_2$ respectively.

Due to the asymmetric configurations of the t-channel gluons, $Q_t \ll k_{it}$, we have, besides $\Delta\eta_i$, a second logarithm $\ln(k_{it}^2/Q_t^2)$ in the BFKL evolution. Using this double log result (that is setting $\Phi(Y_i) = 1$ in (12)), we may simplify expression (17) for $\mathcal{I}$. Then we perform the Q_t^2 and $Q_t'^2$ integrations and find

$$\mathcal{I} \;=\; \frac{1}{(Y_1+Y_2)^2}\int\frac{dt_1}{t_1}\,\frac{dt_2}{t_2}\,\exp\left(-\frac{3\alpha_S}{\pi}\,\Delta\eta\,\left|\ln\frac{t_1}{t_2}\right|\right)\,T\left(\sqrt{|t_1|},\mu\right)\,T\left(\sqrt{|t_2|},\mu\right), \tag{21}$$

where $\Delta\eta$ equals $\Delta\eta_1$ if $|t_1| > |t_2|$, but equals $\Delta\eta_2$ when $|t_1| < |t_2|$.

The luminosity $M^2 d\mathcal{L}/dy dM^2$ calculated from (18) and (6) for inclusive double-diffractive production of a system of mass M and rapidity y is shown in Figs. 2 and 3, by the thin continuous curves corresponding to two choices of rapidity gaps, namely $\Delta\eta_1 = \Delta\eta_2 = 2$ and, $\Delta\eta_1 = \Delta\eta_2 = 3$ in Fig. 1(b). Again we use MRST99 partons [9], to calculate (19). Since we are working at the partonic level, a Monte Carlo simulation would be required to obtain the precise experimental prediction. Unfortunately, the lower curve for $\Delta\eta = 3$ is more relevant, as after hadronization the smaller rapidity gaps with $\Delta\eta = 2$ may be hard to identify.

The effective luminosity, that is the number of gg collisions, is larger for inclusive than exclusive production due to the larger available phase space, since now the transverse momentum of the heavy system M is no longer limited by the proton form factor. Moreover partons of larger k_{ti} tend to have large momentum fractions x_i, see (20). For partons of relatively large x_i we sample mainly the smaller size component of the proton wave function, which in turn has the smaller absorption cross section [4]. This leads to a larger 'soft' survival probability $\hat{S}^2$. To be precise we use model II of Ref. [4] to calculate $\hat{S}^2$. For inclusive production, the survival factor $\hat{S}^2$ depends on the values of M^2 and $\Delta\eta$, since these alter the values of x_i sampled.

2.3 Production via Pomeron-Pomeron fusion

The inclusive process studied in the previous subsection allowed secondary particles in the proton fragmentation regions, see Fig. 1(b). An alternative possibility is to detect both elastically scattered protons, but to permit secondaries in the central rapidity interval $\delta\eta$ containing the heavy system, as schematically sketched in Fig. 1(c). In lowest order perturbative QCD, this process is described by Fig. 6(a), which is similar to Fig. 1(a) for exclusive production. The only difference is that now we have bremsstrahlung associated with the hard subprocess $gg^{PP} \to M$. Therefore we can compute the cross section from the same formula (7), except that the Sudakov-like suppression is weaker. Now the $1-\Delta$ upper limit in the z integration in (10) is specified by

$$\Delta \;=\; \left(\frac{k_t}{\mu + k_t}\right) \cosh\left(\frac{\delta\eta}{2}\right). \tag{22}$$

Clearly the luminosity is larger and increases with $\delta\eta$, as is seen from the dashed curves in Figs. 2, 3 and 4. We label the curves[3] *C-inel.* to indicate *central-inelastic* double-diffractive production of the heavy system, see Fig. 6(a). As can be seen from the figures, we do not gain much luminosity by allowing extra emission in the central region with $\delta\eta = 2$. If we enlarge $\delta\eta$ up to 4 we enhance the luminosity by an order of magnitude, but at a great price, as will now be discussed.

[3]Actually we have included the luminosity of the exclusive process of Fig. 1(a) in the *C-inel.* results. Strictly speaking, therefore, a more precise notation might have been *C-total*, to indicate that the 'elastic' contribution is included.

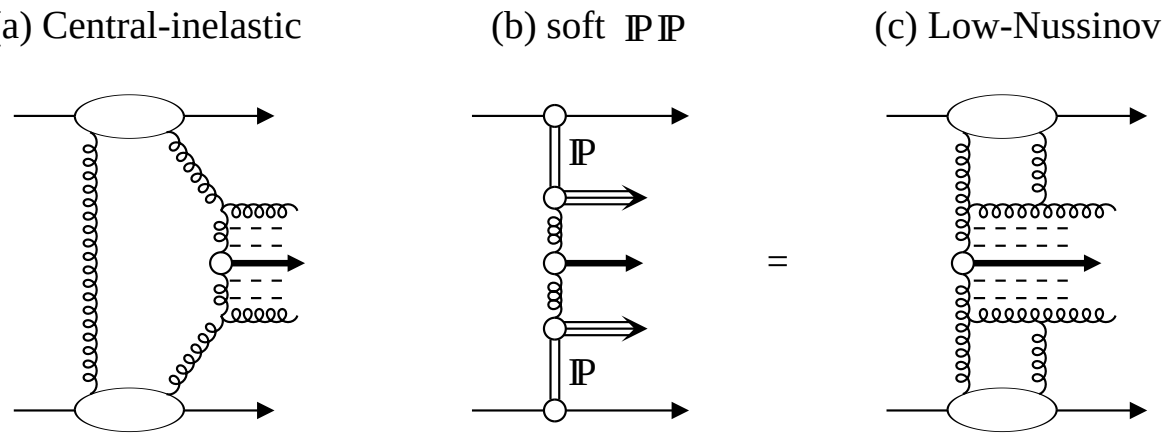

Figure 6: Double-diffractive production of a heavy system, shown by the *bold* central arrow, accompanied by secondaries in the central region, with forward going protons.

First, it is important to note that for processes of the type of Fig. 1(c), the mass M determined by detection of the forward protons is no longer equal to the mass of the heavy system. In this subsection we denote the former mass by M_{PP} and the latter by M_H. We see that $M_{PP} > M_H$ due to the presence of secondaries in the central region. This clearly applies to the process of Fig. 6(a) which we have just discussed, but also to the soft $I\!P I\!P$ fusion process of Fig. 6(b). For these inelastic $I\!P I\!P$ processes we loose all the advantages of the exclusive process. The clean central environment of the heavy system is now populated by secondaries. The mass M_H can therefore no longer be measured by the missing-mass method. Moreover, there is no $J_z = 0$ selection rule to suppress the QCD background.

Since the soft Pomeron-Pomeron fusion process of Fig. 6(b) is at present frequently discussed [12, 13], we study it in more detail to confirm that it is indeed not a viable search mechanism. In terms of Feynman graphs, Fig. 6(b) corresponds to Fig. 6(c) in which the soft Pomerons have been replaced by two-gluon exchange, as originally considered by Low [14] and Nussinov [15]. Interestingly, we see that the cross section for the process in Fig. 6(c) is suppressed by a factor α_S^2 in comparison to that of Fig. 6(a). In the cross section for Fig. 6(b) where, following Ref. [16], the Pomerons are treated as real particles with their own parton distributions, the factor is reflected in the small values of the effective Pomeron structure functions which are determined phenomenologically from diffractive data. It therefore may not be quite so surprising when we show below that the soft Pomeron-Pomeron fusion process of Fig. 6(b) has a *smaller* cross section than exclusive double-diffractive production of Fig. 1(a). The cross section[4] for soft Pomeron-Pomeron fusion was also recently discussed in Ref. [12].

[4]The cross section was also calculated in [13], where a larger value was found, which we cannot reproduce.

The luminosity factor for the soft Pomeron-Pomeron fusion process, shown in Fig. 6(b), is

$$L^{\rm soft} \;=\; \left(\frac{\sigma_0}{16\pi^2}\right)^2 \int dt_1 dt_2\, F_N^2(t_1)\, F_N^2(t_2)\, \left(\frac{1}{x_1}\right)^{2(\alpha(t_1)-1)} \left(\frac{1}{x_2}\right)^{2(\alpha(t_2)-1)}, \tag{23}$$

where we assume the Donnachie-Landshoff parametrization of the elastic pp amplitude [17]

$$\begin{aligned} A_{pp}(s,t) &= i\sigma_0\, F_N^2(t)\, s^{\alpha(t)} \\ \text{Im}\; A(s,t=0) &= s\,\sigma_{\rm tot}(s) \\ \alpha(t) &= 1.08 \,+\, 0.25\, t \end{aligned} \tag{24}$$

with s and t in units of GeV^2. F_N is the proton form factor and $\sigma_0 = 21.7$ mb. The mass and rapidity of the produced system are given by

$$M_{PP}^2 \;=\; x_1\, x_2\, s, \qquad\qquad y \;=\; \frac{1}{2}\,\ln\left(\frac{x_1}{x_2}\right). \tag{25}$$

For this production mechanism the cross section $\hat{\sigma}$ in (3), which multiplies the luminosity, is the standard inelastic cross section given by the convolution of the parton distributions (of the Pomerons) $a_i^{I\!P}$ with the cross section for the $a_1 a_2 \to M$ hard subprocess

$$\hat{\sigma} \;=\; \sum_{a_1,a_2} \int \frac{dz_1}{z_1} \int \frac{dz_2}{z_2}\, z_1 a_1^{I\!P}(z_1)\, z_2 a_2^{I\!P}(z_2)\, \sigma(a_1 a_2 \to M), \tag{26}$$

with $a = g, q$. To estimate $\hat{\sigma}$ we assume gluon dominance and that $z g^{I\!P}(z) \simeq 0.7$ for our kinematic domain, which is consistent with the distribution obtained by the H1 collaboration from the analysis of their diffractive data [18]. Then (26) gives

$$\begin{aligned} \hat{\sigma} &\simeq (0.7)^2\, \sigma(gg \to M) \int \frac{dz_1}{z_1} \int \frac{dz_2}{z_2} \\ &\simeq (0.7)^2\, \sigma(gg \to M)\, (\delta y)^2/2, \end{aligned} \tag{27}$$

where

$$\delta y \;=\; \ln(M_{PP}^2/M_H^2). \tag{28}$$

Here, to be definite, we have assumed that the heavy system M is a Higgs boson of mass M_H. Next, it is important to note that $\sigma(gg \to H)$ for the inelastic subprocess within the soft $I\!P I\!P$ fusion mechanism of Fig. 6(b) is a factor $1/2(N_C^2-1)$ *smaller* than the corresponding $\sigma(gg \to H)$ for the exclusive process of Fig. 1(a). Recall that this factor arises because the exclusive process proceeds via the *coherent* fusion of gluons of different spin and colour, which leads to an enhancement of $2(N_C^2-1)$ in comparison with the inclusive process of Fig. 6(b), see (4) and (5).

In addition, at Tevatron energies, after observing the leading outgoing proton and antiproton, the available phase space δy becomes rather small, $\delta y \sim 1$. In summary, the cross section $\hat{\sigma}$ multiplying the luminosity in (3) is a factor of about

$$(0.7)^2 \, \frac{1}{2(N_C^2-1)} \, \frac{(\delta y)^2}{2} \; \simeq \; \frac{1}{64} \tag{29}$$

smaller for production via soft $I\!P I\!P$ fusion (Fig. 6(b)) than via the 'clean' exclusive process of Fig. 1(a). Now from Fig. 3, we see that, for the production of a Higgs boson of mass $M_H = 120$ GeV, the soft $I\!P I\!P$ luminosity calculated from (23) is only a factor of about 10 larger than the luminosity for exclusive production. In both processes we use the same survival factor[5] $\hat{S}^2$, which was given at the end of subsection 2.1. Thus we obtain our advertised result: the expected rate of double-diffractive Higgs production at the Tevatron in the 'dirty' environment of inelastic $I\!P I\!P$ fusion (Fig. 6(b)) is in fact *smaller*[6] than the rate for production by the 'clean' exclusive process of Fig. 1(a).

Of course, at LHC energies the available phase space δy is larger. Recall, from (27), $\hat{\sigma}$ grows as $(\delta y)^2$. On the other hand, in going from Tevatron to LHC energies, the ratio of the exclusive to soft $I\!P I\!P$ luminosities increases by more than an order of magnitude (see Fig. 2), due to the growth of gluons at small x. We conclude that there is nothing to be gained by studying the soft $I\!P I\!P$ fusion mechanism, at least from the point of view of Higgs searches.

2.4 Production via $\gamma\gamma$ and WW fusion

For completeness we give the luminosity factors assuming that the rapidity gaps are due to the production of the (M, y) system via $\gamma\gamma$ and WW fusion. We have

$$L^{\gamma\gamma} \; = \; \left(\frac{\alpha}{\pi}\right)^2 \int_{t_{1,\,\min}} dt_1 \frac{(t_1 - t_{1,\,\min})}{t_1^2} \; (F^{\rm em}(t_1))^2 \int_{t_{2,\,\min}} dt_2 \frac{(t_2 - t_{2,\,\min})}{t_2^2} \; (F^{\rm em}(t_2))^2 \, , \tag{30}$$

where $|t_{i,\min}| = x_i^2 m_N^2$, m_N is the proton mass and $\alpha = 1/137$. As the dominant (logarithmically enhanced) contribution comes from very small $|t_i|$, that is large impact parameters, here we would expect the survival factor $\hat{S}^2$ to be close to 1 [5]. Indeed, we find this to be the case, as illustrated by the values of $\hat{S}^2$ that are given in Section 3.1.3 for Higgs production via $\gamma\gamma$ fusion. The $\gamma\gamma$ luminosity, (6), shown in Fig. 2 is calculated[7] from $L^{\gamma\gamma}$, and includes the gap survival factor $\hat{S}^2$.

[5] Another way to estimate $\hat{S}^2$ is to compare the data with the theoretical prediction which does not account for the soft rescattering effects. Special care should be taken if this method is used. If the 'bare' theoretical cross section is calculated using, for example, only the mechanism of Fig. 6(b) and does not include the more important central inelastic production mechanism of Fig. 6(a), then $\hat{S}^2 =$ data/theory will be overestimated.

[6] This estimate of the soft Pomeron-Pomeron contribution is in reasonable agreement with that of Ref. [12].

[7] Besides the proton form factor $F_1^{\rm em}$, we also include the small contribution from $F_2^{\rm em}$, when we evaluate $F^{\rm em}(t)$ in (30).

The effective luminosity for producing the (M, y) system by WW fusion is given by

$$L^{WW} = \left[\int_{x_1^{\min}}^1 U(x_1)\,\frac{dx_1}{x_1}\int_{x_2^{\min}}^1 D(x_2)\,\frac{dx_2}{x_2} + \int_{x_1^{\min}}^1 D(x_1)\,\frac{dx_1}{x_1}\int_{x_2^{\min}}^1 U(x_2)\,\frac{dx_2}{x_2}\right] \times \left(\frac{g^2}{16\pi^2}\right)^2 \int \frac{dt_1 M_W^2}{(M_W^2 - t_1)^2}\,\frac{dt_2 M_W^2}{(M_W^2 - t_2)^2}, \tag{31}$$

where $g^2 = 8M_W^2 G_F/\sqrt{2}$ and M_W is the mass of the W boson. The lower limits of the integrations are given by (20). The effective parton densities, $U(x_i, k_{it}^2)$ and $D(x_i, k_{it}^2)$ are

$$\begin{aligned} U(x) &= xu + x\bar{d} + x\bar{s} + xc \\ D(x) &= x\bar{u} + xd + xs + x\bar{c}. \end{aligned} \tag{32}$$

The survival factor $\hat{S}^2$ is calculated using the two-channel eikonal approach described in Ref. [4]. We use the more realistic model II [4], as in Section 2.2.

Predictions for the WW luminosity are shown in Figs. 3, 4 and 7. Since WW fusion can only mediate inclusive production, the missing mass technique cannot be used. However, here, the enlargement of the rapidity gaps does not reduce the luminosity as much as it did for gg fusion. Fig. 7 shows the WW luminosity for $\Delta\eta = 2$ and $\Delta\eta = 3$, in comparison with that for conventional inelastic production via WW fusion for which $\Delta\eta = 0$. These results should be compared with the results for gg fusion in Figs. 3 and 4. The upper (dotted) curve shows the inelastic luminosity ($\Delta\eta = 0$) assuming that the gg pair are in a colour singlet state. If this luminosity is compared with the inclusive luminosity for the production of a $M = 120$ GeV system with rapidity gaps of $\Delta\eta = 3$ on either side, then we loose a factor of 10^{-3} at LHC energies, while the corresponding ratio for production via WW fusion is only 0.02. Production by WW fusion is less suppressed with increasing $\Delta\eta$ for two reasons. First, since the W bosons originate mainly from valence quarks, that is the component of the proton wave function with the smaller absorption cross section, the soft survival probability of the rapidity gaps, $\hat{S}^2$, is larger. Secondly, as the W boson is a colourless object, there is no Sudakov suppression due to QCD bremsstrahlung.

3 Cross sections for the hard subprocesses and for double-diffractive production

Selecting double-diffractive events means essentially that we are working with a gluon-gluon collider[8]. Indeed, the luminosities presented in Section 2 were given in terms of the numbers

[8]For completeness, we also consider production mechanisms where the rapidity gaps are associated with $\gamma\gamma$ and WW fusion processes.

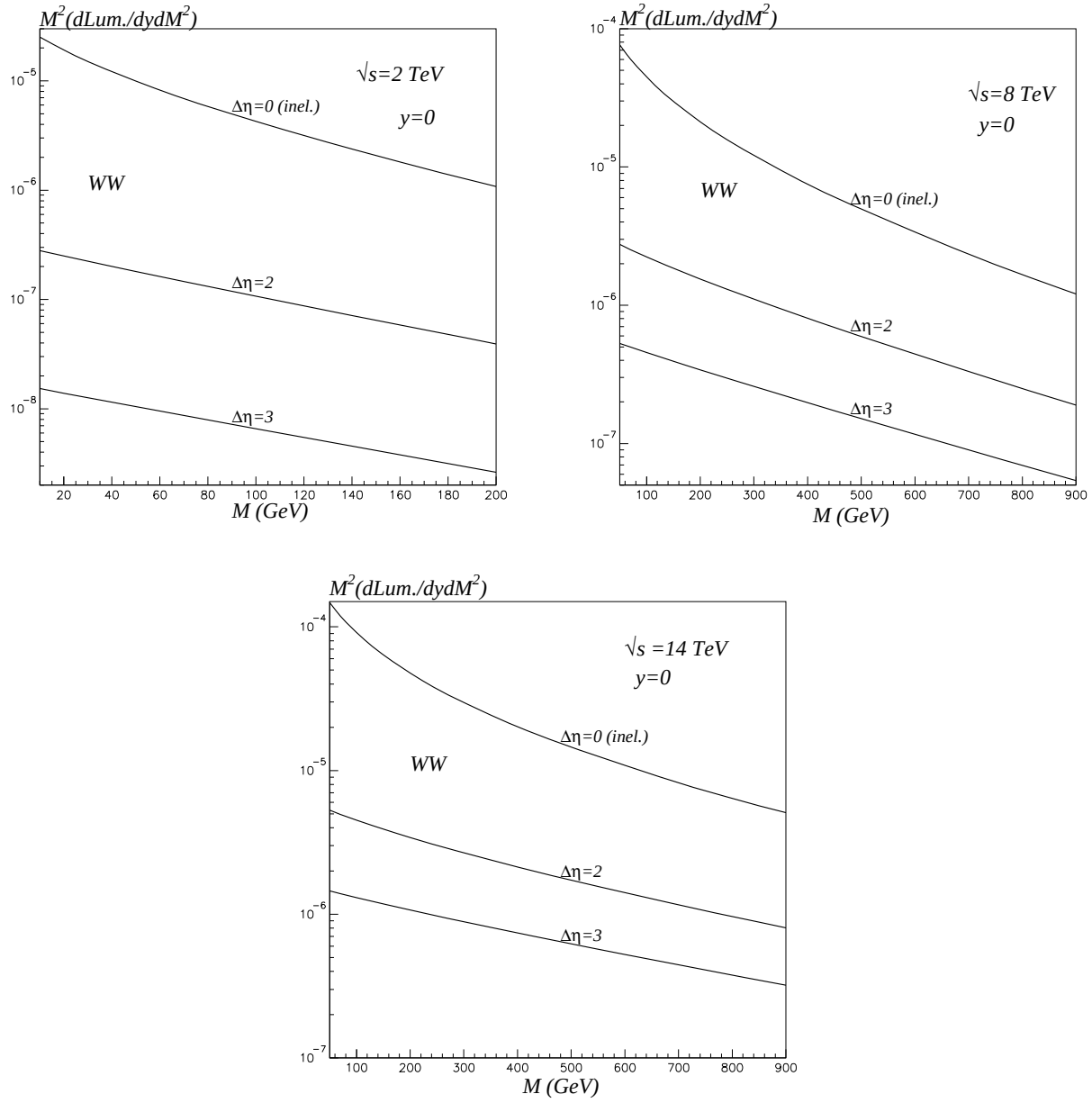

Figure 7: The luminosity $M^2\partial\mathcal{L}/\partial y\partial M^2$ versus M for the production of a heavy system at $y = 0$ by WW fusion, with a rapidity gap of size $\Delta\eta$ on either side, at pp or $p\bar{p}$ collider energies of $\sqrt{s} = 2, 8$ and 14 TeV.

of gg collisions per proton-proton interaction. As emphasized before, there is an important distinction between exclusive and inclusive double-diffractive production of a heavy system M. In *exclusive* events the forward protons select a colour singlet, $J_z = 0$ incoming gg state. In *inclusive* events the $J_z = 0$ selection rule is absent. Therefore, to predict the cross section

(or event rate at the collider) we have to be careful to ensure that we multiply the relevant luminosity by the appropriate $gg^{PP} \to M$ subprocess cross section. Recall that the PP superscript was to indicate that the gluons are mediating a double-diffractive process (loosely called Pomeron-Pomeron production).

In this section we give the subprocess cross sections $d\hat{\sigma}/d\Omega$ which are relevant to the double-diffractive production of various heavy systems M. The differential form is symbolic. For example, for the production of a dijet system, with a rapidity gap on either side, we study $d\hat{\sigma}/dE_T^2$, where E_T is the transverse energy of the jets. In this way we can readily predict the cross sections for double-diffractive production at various collider energies, using

$$M^2 \frac{d\sigma^{(i)}}{dydM^2d\Omega} = \left(M^2 \frac{d\mathcal{L}^{(i)}}{dydM^2} \right) \frac{d\hat{\sigma}^{(i)}(M^2)}{d\Omega}, \tag{33}$$

see (3). The expression in brackets is the luminosity calculated in Section 2, which is to be multiplied by the appropriate subprocess cross section, which we enumerate below. We study in turn, resonance production (e.g. Higgs, χ_b), dijet production, $\gamma\gamma$ production, $t\bar{t}$ production, the production of SUSY particles (e.g. $\tilde{g}\tilde{g}, \tilde{q}\bar{\tilde{q}}$), and various soft phenomena.

3.1 Resonance production

The subprocess cross section for the double-diffractive production of a 0^{++} resonance R may be written in terms of its two-gluon partial width

$$\hat{\sigma}^{\rm excl}(gg^{PP} \to R) = \frac{2\pi^2 \tilde{\Gamma}(R \to gg)}{M_R^3} \, \delta\left(1 - \frac{M^2}{M_R^2}\right), \tag{34}$$

$$\hat{\sigma}^{\rm incl} = \frac{1}{2} \, \hat{\sigma}^{\rm excl}. \tag{35}$$

The extra factor of $\frac{1}{2}$ arises in inclusive double-diffractive production due to the absence of the $J_z = 0$ selection rule in this case. It reflects the spin coherence of the *exclusive* process where the incoming gluon polarisations are correlated, whereas for *inclusive* production, the cross section is averaged over the incoming spins in the usual way, that is

$$\hat{\sigma}^{\rm excl} \sim |\overline{\mathcal{M}}|^2, \qquad \hat{\sigma}^{\rm incl} \sim \overline{|\mathcal{M}|^2}. \tag{36}$$

3.1.1 Higgs production

In the Born approximation, the width $\tilde{\Gamma}$ in (34) is just the lowest order $R \to gg$ decay width Γ_0. For Higgs production we include the NLO correction to $\hat{\sigma}(gg \to H)$, using

$$\begin{aligned} \tilde{\Gamma}(H \to gg) &= \Gamma_0(H \to gg) \left(1 + \frac{\alpha_S(M_H)}{\pi} \left(\pi^2 + \frac{11}{2}\right)\right) \\ &\simeq 1.5 \, \Gamma_0(H \to gg). \end{aligned} \tag{37}$$

Note that (37) is not the complete NLO correction to the $H \to gg$ partial width, since it does not include the contribution from the emission of QCD radiation, see, for example, [19, 20]. For a Higgs boson of mass $M_H = 120$ GeV, we obtain from (34) and (37)

$$\hat{\sigma}^{\rm excl} \;\simeq\; \delta \left(1 \;-\; \frac{M^2}{M_H^2}\right) \; 1.1 \text{ pb}. \tag{38}$$

In the intermediate mass range of the Higgs, $\hat{\sigma}$ depends weakly on M_H, as $\Gamma_0 \sim M_H^3 \alpha_S^2(M_H)$ largely cancels the M_H^{-3} factor in (34).

Given the subprocess cross section (38) and the luminosities of Figs. 2, 3 and 4, we can readily predict the cross section for double-diffractive Higgs production at the LHC and the Tevatron. To be specific let us take $M_H = 120$ GeV. Then from Fig. 3 we have

$$\begin{aligned} \left.\frac{d\mathcal{L}}{dy}\right|_{y=0} &\simeq 0.6 \times 10^{-3} \text{ (LHC)} \\ &\simeq 0.9 \times 10^{-4} \text{ (Tevatron)}. \end{aligned} \tag{39}$$

Also we see that for Higgs production $\Delta y \simeq 5$ (LHC) or 2 (Tevatron) will allow a quick estimate of the y integration. Finally multiplying by $\hat{\sigma}$ of (38) (which takes care of the M^2 integration), we obtain

$$\begin{aligned} \sigma(pp \to p + H + p) &\simeq 3 \text{ fb (LHC)} \\ \sigma(p\bar{p} \to p + H + \bar{p}) &\simeq 0.2 \text{ fb (Tevatron)}. \end{aligned} \tag{40}$$

These predictions are consistent with our previous estimates [5]. The background to this signal for the Higgs boson is discussed in Section 3.2.3.

3.1.2 χ_b production

Another interesting example is $\chi_b(0^{++})$ resonance production, see, for example, [21, 2, 22]. Again $\hat{\sigma}$ is given by (34), with [23]

$$\tilde{\Gamma}(\chi_b \to gg) \;=\; \Gamma_0(\chi_b \to gg) \; \left(1 + 9.8 \, \frac{\alpha_S}{\pi}\right) \;=\; 550 \text{ keV}, \tag{41}$$

where we have used the lattice result $\Gamma_0 = 354$ keV [24]. This gives

$$\hat{\sigma}^{\rm excl} \;\simeq\; \delta \left(1 \;-\; \frac{M^2}{M_\chi^2}\right) \; 3.8 \text{ nb}. \tag{42}$$

As an example, consider χ_b production at the Tevatron. From Fig. 2 we have

$$\left.\frac{d\mathcal{L}}{dy}\right|_{y=0} \;\simeq\; 1.6 \times 10^{-2}, \qquad \Delta y \;\simeq\; 2, \tag{43}$$

which combined with (42) gives

$$\sigma(p\bar{p} \to p + \chi_b + \bar{p}) \;\simeq\; 120 \text{ pb}, \tag{44}$$

consistent with the predictions of Ref. [2].

3.1.3 Higgs production via $\gamma\gamma$ and WW fusion

For completeness we estimate Higgs production by $\gamma\gamma$ and WW fusion. For $\gamma\gamma$ fusion, (34) is replaced by

$$\hat{\sigma}(\gamma\gamma \to H) \;=\; \frac{8\pi^2\tilde{\Gamma}(H\to\gamma\gamma)}{M_H^3}\,\delta\left(1\;-\;\frac{M^2}{M_H^2}\right). \tag{45}$$

The factor of 8, in place of 2, arises because for coloured gluons there was an extra factor of $(N_C^2-1)^{-1}$ due to colour averaging and the absence of the $J_z=0$ selection rule. For $M_H = 120$ GeV we have $\tilde{\Gamma}(H\to\gamma\gamma)\simeq 7.9$ keV, and so

$$\hat{\sigma}(\gamma\gamma \to H) \;\simeq\; \delta\left(1\;-\;\frac{M^2}{M_H^2}\right)\,0.1\text{ pb}. \tag{46}$$

The $\gamma\gamma$ luminosity, integrated over y, is 1.0×10^{-4} and 1.1×10^{-3} at the Tevatron and LHC respectively, which leads to the cross sections

$$\begin{aligned}\sigma(p\bar{p}\to p+H+\bar{p})_{\gamma\gamma} \;&\simeq\; 0.01\text{ fb} \qquad \text{(Tevatron)}\\ \sigma(pp\to p+H+p)_{\gamma\gamma} \;&\simeq\; 0.1\text{ fb} \qquad \text{(LHC)}.\end{aligned} \tag{47}$$

Recall that the $\gamma\gamma$ luminosity includes the gap survival factor $\hat{S}^2$, which we calculate to be 0.75 and 0.9 at Tevatron and LHC energies respectively for the production of a Higgs of mass $M_H = 120$ GeV. The cross sections (47) of the present, more detailed, calculation are lower than previous results which were derived in the leading log approximation with $\hat{S}^2=1$ [25, 5, 26].

Note that the strong and electromagnetic contributions to exclusive Higgs production (with rapidity gaps) have negligible interference, because they occur at quite different values of the impact parameter. Also, it is worth mentioning that the $\gamma\gamma\to H$ fusion mechanism provides a natural lower limit for the Higgs exclusive production rate.

For Higgs production via WW fusion

$$\begin{aligned}\hat{\sigma}^{\rm incl}(WW\to H) \;&=\; \frac{\pi g^2 M_W^2}{M_H^4}\,\delta\left(1\;-\;\frac{M^2}{M_H^2}\right)\\ &\simeq\; \delta\left(1\;-\;\frac{M^2}{M_H^2}\right)\,16\text{ nb}\end{aligned} \tag{48}$$

for $M_H = 120$ GeV. The coupling $g^2 = 8M_W^2G_F/\sqrt{2}$.

Of course, WW fusion only mediates inclusive Higgs production. Note that there is almost no interference between the WW and gg^{PP} fusion mechanisms. Recall that the former process produces Higgs with high transverse momentum, and as such may give a viable signal [27, 28, 29]. Moreover, if we select events with rapidity gaps we suppress the QCD $b\bar{b}$ background, while paying less price for the gaps in WW fusion as compared to those in gg fusion (as discussed at the end of Section 2.4).

3.2 Dijet production

The Born cross sections, for *colour-singlet* production of a dijet system of mass M, are (see, for example, [30, 31, 32, 10])

$$\frac{d\hat{\sigma}^{\rm excl}}{dt}(gg^{PP}\to gg) \;=\; \frac{9}{4}\,\frac{\pi\alpha_S^2}{E_T^4}, \tag{49}$$

$$\frac{d\hat{\sigma}^{\rm excl}}{dt}(gg^{PP}\to q\bar{q}) \;=\; \frac{\pi\alpha_S^2}{6E_T^4}\,\frac{m_q^2}{M^2}\,\beta^2, \tag{50}$$

$$\frac{d\hat{\sigma}^{\rm incl}}{dt}(gg^{PP}\to gg) \;=\; \frac{9}{2}\,\frac{\pi\alpha_S^2}{E_T^4}\,\left(1\,-\,\frac{E_T^2}{M^2}\right)^2, \tag{51}$$

$$\frac{d\hat{\sigma}^{\rm incl}}{dt}(gg^{PP}\to q\bar{q}) \;=\; \frac{\pi\alpha_S^2}{E_T^2M^2}\,\frac{1}{6}\left[\left(1\,-\,\frac{2E_T^2}{M^2}\right)\left(1\,-\,\frac{2m_q^2}{E_T^2}\right)\,+\,\frac{m_q^2}{E_T^2}\,(1+\beta^2)\right], \tag{52}$$

where E_T is the transverse energy of the jets and $\beta=\sqrt{1-4m_q^2/M^2}$. We choose the scale of α_S to be $M/2$ to be consistent with the convention we have used for the luminosities in Section 2. For $M^2\gg E_T^2$ we see, that contrary to 0^{++} resonance production (35), gg production is a factor 2 larger in the inclusive as compared to the exclusive process. This is the result of averaging over the polarisations of the incoming gluons, (5). Moreover we see that the Born cross section (50) for exclusive $gg^{PP}\to q\bar{q}$ production vanishes as $m_q\to 0$ [32, 33], which is a consequence of the $J_z=0$ selection rule for the gluon polarizations [2, 10].

Rather than working in terms of the subprocess variables M^2 and t, it is often convenient to use E_T^2 and $\delta\eta_j$, where $\delta\eta_j=\eta_1-\eta_2$ is the difference in rapidities of the two outgoing jets. It turns out that factors in the Jacobian cancel, so that we obtain the relatively simple relation [10]

$$\frac{d\hat{\sigma}}{dt}\Big/\frac{dM^2}{M^2} \;=\; \frac{d\hat{\sigma}}{dE_T^2}\Big/d(\delta\eta_j). \tag{53}$$

Thus the product of the luminosity (shown in Figs. 2, 3 and 4) and $d\hat{\sigma}/dt$, will give an evaluation of the differential cross section $d\sigma/dyd(\delta\eta_j)dE_T^2$.

The large cross section for exclusive dijet production provides the first opportunity of experiment to check the double-diffractive predictions, already at the Tevatron. For example, let us calculate the event rate for jets in the domain defined by the intervals $25<E_T<35$ GeV and $\delta\eta_j<2$. If we integrate (49) over these intervals, and multiply by the luminosity $\partial\mathcal{L}/\partial y\simeq 3\times10^{-4}$ appropriate to $M=2E_T\cosh(\delta\eta_j/2)\simeq 70$ GeV, then we obtain

$$\Delta\sigma(p\bar{p}\to p+jj+\bar{p}) \;\simeq\; 60\ {\rm pb} \tag{54}$$

corresponding to jets with $25<E_T<35$ GeV and $|\eta_1-\eta_2|<2$, which is in qualitative agreement with previous results [10, 5]. Thus even for a Tevatron luminosity of 1 fb^{-1}, we estimate there should be 60,000 exclusive events in this particular domain.

3.2.1 Dijets as a luminosity monitor

There are, of course, uncertainties in our estimates of the cross sections for double-diffractive processes. First, the calculation of the soft survival factor $\hat{S}^2$ is based on a simplified two-channel eikonal model [3, 4]. With the presently available soft diffractive data, these estimates of $\hat{S}^2$ are as good as possible, but it is hard to guarantee the precision of predictions which rely on soft physics. Secondly recall, from Section 2, that the luminosity was calculated in terms of the unintegrated, skewed gluon distribution f_g, and that $\mathcal{L} \propto f_g^4$. Thus a 20% uncertainty in f_g results in a factor of 2 uncertainty in the luminosity. We calculated f_g in terms of the conventional gluon distribution obtained from the results of a global parton analysis of deep inelastic and related hard scattering data [9]. However the prescription is only justified at leading order and for small x [8, 7]. In the present paper we use an improved formula for f_g [7], and as a result the double-diffractive luminosity at Tevatron energies become a factor of two larger than in Ref. [5][9]. However the same luminosity determines the cross sections for different double-diffractive processes. Thus dijet production, where the cross section is largest, offers an excellent way to monitor the gg^{PP} luminosity [5].

3.2.2 Dijets as a gluon factory

Another application of the large rate of exclusive dijet production is as a gluon factory. The remarkable purity of the colour-singlet, $J_z = 0$, di-gluon system provides a unique environment to study high energy gluon jets [2].

3.2.3 Dijets as a background to the Higgs signal

The large dijet production rate may produce a huge background to the Higgs $H \to b\bar{b}$ signal. Recall that the cross section for exclusive double-diffractive Higgs production was calculated in Section 3.1.1.

In fact, for any 0^{++} resonance the ratio of the exclusive $R \to gg$ signal to the gg background is

$$\frac{S_{gg}}{B_{gg}} \;=\; \frac{4\pi}{9(9.7)\,\alpha_S^2\,\Delta M}\,\Gamma\left(R \to gg^{J_z=0}\right), \tag{55}$$

where ΔM is the experimental missing-mass resolution, the scale of α_S is $M/2$ and the factor 9.7 comes from imposing a cut $60^\circ < \theta^* < 120^\circ$ in order to improve the signal-to-background ratio. θ^* is the decay angle in the dijet rest frame. Note that the major part of NLO effects and uncertainties in the luminosity cancel in ratio (55).

[9]The unintegrated skewed gluon distribution $f_g(x, x', Q_t^2, \mu^2)$ has been tested, both by providing a successful description of the data on diffractive vector meson production at HERA [34] and by agreement with the upper bound on diffractive dijet production at the Tevatron [35, 1]. However in both cases a much lower scale is probed and we did not need precision better than 20–30%.

For $H \to b\bar{b}$, the signal-to-QCD background ratio is

$$\frac{S(gg^{PP} \to b\bar{b})}{B(gg^{PP} \to gg)} \;\simeq\; 4.3 \times 10^{-3}\,\mathrm{Br}(H \to b\bar{b})\,\left(\frac{M}{100\ \mathrm{GeV}}\right)^3\,\left(\frac{250\ \mathrm{MeV}}{\Delta M}\right), \tag{56}$$

which is very small [2]. Fortunately, if we tag the b and $\bar{b}$ jets to reject the gg events, we can strongly suppress the QCD background. Recall that the $gg^{PP} \to b\bar{b}$ QCD background process is suppressed by colour and spin factors, and by the $J_z = 0$ selection rule. In this way the background is suppressed by an extra factor

$$\frac{m_b^2}{M_H^2}\,\frac{1}{4}\,\frac{1}{27} \;\lesssim\; 2 \times 10^{-5}. \tag{57}$$

However the full suppression is only true in the Born approximation. Recall that large angle gluon radiation in the final state violates the $J_z = 0$ selection rule [36], so in the $b\bar{b}$ QCD background the suppression factor m_b^2/M_H^2 is replaced by α_S/π. The final result for the $H \to b\bar{b}$ signal-to-background ratio is therefore

$$\frac{S(gg^{PP} \to H \to b\bar{b})}{B(gg^{PP} \to b\bar{b})} \;\gtrsim\; 15\left(\frac{250\ \mathrm{MeV}}{\Delta M}\right), \tag{58}$$

for a Higgs boson of mass $M_H = 120$ GeV.

3.3 Double-diffractive $\gamma\gamma$ production

At first sight, the subprocess $gg^{PP} \to \gamma\gamma$ appears attractive to serve as an alternative gg^{PP} luminosity monitor for the exclusive double-diffractive processes[10]. However it turns out that the event rate is too small. Using the known results[11] for the QED $\gamma\gamma \to \gamma\gamma$ helicity amplitudes [37], we calculate the $J_z = 0$, parity $P = +1$ subprocess cross section to be

$$\hat{\sigma}(30^\circ < \theta^*_\gamma < 150^\circ) \;\simeq\; 0.3(0.04)\ \mathrm{pb} \tag{59}$$

for $M_{\gamma\gamma} \sim 50(120)$ GeV. When multiplied by the luminosity at the Tevatron of $1.8 \times 10^{-3}(2 \times 10^{-4})$, we obtain, assuming $\int dM^2/M^2 \simeq 1$,

$$\sigma(p\bar{p} \to p + \gamma\gamma + \bar{p}) \;\simeq\; 0.5\ \mathrm{fb}\ (0.008\ \mathrm{fb}). \tag{60}$$

On the other hand, for the LHC for $M_{\gamma\gamma} \simeq 120$ GeV we expect

$$\sigma(pp \to p + \gamma\gamma + p) \;\simeq\; 0.12\ \mathrm{fb}. \tag{61}$$

Note that for $M_{\gamma\gamma} \simeq 120$ GeV the observable rate of Standard Model exclusive $\gamma\gamma$ events is expected to be much less than even Higgs $\to b\bar{b}$ signal. In comparison to exclusive $gg^{PP} \to gg$ subprocess, the $gg^{PP} \to \gamma\gamma$ rate is smaller by a factor of 10^6 for $E_{Tg} \simeq E_{T\gamma}$.

[10]We are grateful to Mike Albrow and Beate Heinemann for discussions on this proposal.

[11]We thank Andrei Shuvaev for checking various formulae for $\gamma\gamma$ production.

This obvious disadvantage of the Standard Model exclusive diphoton production can be turned into an attractive advantage for searches at hadronic colliders of signs of the existence of extra dimensions, which for instance appear in theories of low-scale gravity [38]. The small background rate, induced by the conventional box diagram contribution, may allow a very sensitive high-mass diphoton probe of the effective scale of quantum gravity effects, M_S (see, for example, [39, 40]). To illustrate the level of the possible signal we follow the estimates of Ref. [39] with effective scale $M_S = 1.5$ TeV. At $M_{\gamma\gamma} \sim 500$ GeV one then would expect, for $30^\circ < \theta^*_\gamma < 150^\circ$,

$$\hat{\sigma}^{\rm incl}_{\rm extra\ dim.} \ \sim \ F^2 \left(\int \frac{dM^2}{M^2} \right) 50 \text{ fb}, \tag{62}$$

where the factor F is given by (see, for example, [39])

$$F \ = \ 2/(n-2) \quad \text{for} \quad n \ > \ 2, \tag{63}$$

where n is the number of extra (compactified) dimensions. We consider here the inclusive configuration of Fig. 1(b), since for exclusive LO kinematics there is no $J_z = 0$ point-like gluon-gluon coupling to a 2^+ "graviton".

Taking $\int dM^2/M^2 \sim 1$, after multiplying by the double-diffractive inclusive luminosity of 2×10^{-3} (for $\Delta\eta = 3$), we would expect at the LHC

$$\Delta\sigma_{\rm extra\ dim.}(pp \to X + \gamma\gamma + Y) \ \sim \ 0.1 F^2 \text{ fb}, \tag{64}$$

which, assuming that F^2 is of order 1, should yield about 10 events, for an integrated luminosity of $\mathcal{L} = 100$ fb^{-1}. It is quite possible that future Tevatron results may increase the existing lower limit on M_S, and hence make a diphoton signature for extra dimensions invisible.

Of course, in the inclusive configuration, there may be some additional background induced by $\gamma\gamma$ emission off the quark lines in the process where the rapidity gaps are created by colourless $q\bar{q}$ t-channel exchange. However for gaps with $\Delta\eta = 3$, a preliminary estimate[12] shows that this quark contribution does not exceed the background contribution coming from the $gg \to \gamma\gamma$ box diagram. Thus the total background should not be greater than about 5–10%.

3.4 $t\bar{t}$ production

The exclusive double-diffractive production of $t\bar{t}$ pairs may provide new opportunities for studying top quark physics. In particular, it offers a novel probe of the QCD dynamics in the $t\bar{t}$ system. The Born cross section is given by (50). Due to parity conservation, the $t\bar{t}$ pair is produced in a P-wave state, and so the threshold behaviour goes as β^3, where β is the quark velocity in the $t\bar{t}$ rest frame. Of course, the Born cross section is modified by Coulomb and top-quark width effects [41, 42], but for illustration it is sufficient to neglect these, see our estimates at the end of subsection 3.5.2.

Note that the observation of $t\bar{t}$ exclusive production can be used as a template of the ability of the missing mass method to find signals of New Physics.

[12] We plan to study $q\bar{q}$ exchange in more detail in the future.

3.5 SUSY particle production

Double-diffractive exclusive processes, in principle, provide a unique opportunity to investigate the whole of the strong interaction sector of physics beyond the Standard Model. As an example, we consider supersymmetry, which is a front-runner in searches for New Physics. Here we ignore the current theoretical SUSY prejudices and assume for illustration, first, that the gluino is the lightest supersymmetric particle (LSP). The second scenario that we consider is that unstable gluinos and squarks exist with masses close to the current experimental limits. Note that it is difficult to separate gluinos and squarks produced in standard inelastic hadronic collisions. Moreover, gluino studies appear especially promising in gg collisions since these cannot be easily achieved at linear e^+e^- colliders.

3.5.1 Gluinoball production

In recent publications [43] an interesting possibility is discussed that a gluino $\tilde{g}$ is the LSP (or next-to-LSP) or, to be specific, that it does not decay within the detector. The allowed mass window is claimed to be 25–35 GeV. Within such a scenario there should exist a spectrum of $\tilde{g}\tilde{g}$ bound states (gluinoballs or gluinonia), which may reveal themselves in gluon-gluon collisions. The orbital angular momentum L must be odd in such gg^{PP} collisions, due to parity conservation. Therefore the lowest lying colourless bound states is the $0^{++}(^3P_0)$ state, which we denote $\tilde{G}$, with principal quantum number $n = 2$. Relative to the $2m_{\tilde{g}}$ threshold, the energies of such P-wave $\tilde{g}\tilde{g}$ bound states are

$$E_n \;=\; -\,\frac{9}{4}\,m_{\tilde{g}}\,\frac{\alpha_S^2}{n^2} \tag{65}$$

with $n \geq 2$, where α_S is to be evaluated at the Coulombic scale $k_G = 3\alpha_S m_{\tilde{g}}/2$ (see, for example, [44, 45]). We may estimate the partial width of the $\tilde{G} \to gg$ decay using the Coulombic approximation. The old results of the two-photon decay of P-wave positronium [46] may be applied (see, for example, [44, 45]), which gives

$$\begin{aligned} \Gamma(\tilde{G} \to gg) \;&=\; 6.4\,\alpha_S^2(m_{\tilde{g}})\,\alpha_S^5(k_G)\,M_{\tilde{G}} \\ &\simeq\; \left[\frac{M_{\tilde{G}}}{60\ \text{GeV}}\right]\,0.2\ \text{MeV}, \end{aligned} \tag{66}$$

where $M_{\tilde{G}} \approx 2m_{\tilde{g}}$. Then, on using (34), we obtain

$$\hat{\sigma}^{\text{excl}}(gg^{PP} \to \tilde{G}) \;=\; \delta\left(1 \,-\, \frac{M^2}{M_{\tilde{G}}^2}\right)\ 18\ \text{pb}. \tag{67}$$

The anticipated cross section for the signal is quite sizeable. For example, for $M_{\tilde{G}} = 60$ GeV,

$$\begin{aligned} \sigma(pp \to p + \tilde{G} + p) \;&\simeq\; 0.4\ \text{pb (LHC)}, \\ \sigma(p\bar{p} \to p + \tilde{G} + \bar{p}) \;&\simeq\; 20\ \text{fb (Tevatron)}. \end{aligned} \tag{68}$$

However the signal-to-background ratio is

$$\frac{S(gg^{PP} \to \tilde{G} \to gg)}{B(gg^{PP} \to gg)} \;=\; 0.6 \times 10^{-2} \left(\frac{250 \text{ MeV}}{\Delta M}\right) \left(\frac{M_{\tilde{G}}}{60 \text{ GeV}}\right), \tag{69}$$

which makes detection difficult, even with angular cuts. Some words of caution are in order here. Our estimates are based simply on the lowest-order Coulombic formula, (66). More refined calculations of $\Gamma(\tilde{G} \to gg)$ are certainly needed. Secondly, we have neglected the possible interference between the signal and the background.

The threshold production of (quasi) stable gluino pairs may be strongly affected by QCD final-state interactions, in analogy to the celebrated Coulomb threshold phenomena in QED [47]. As follows from the results of Refs. [42, 45], in the zero-width approximation the P-wave threshold cross section, $d\sigma_P(\tilde{g}\tilde{g}; M)$, is

$$d\sigma_P(\tilde{g}\tilde{g}; M) \;=\; d\sigma_P^{(0)}(\tilde{g}\tilde{g}; M)\, |\psi_{\tilde{g}}(0)|^2 \left(1 \,+\, \frac{Z_g^2}{4\pi^2}\right), \tag{70}$$

where $d\sigma_P^{(0)}(\tilde{g}\tilde{g}, M)$ denotes the Born cross section at cm energy $M \geq 2m_{\tilde{g}}$. $\psi_{\tilde{g}}(0)$ is the Coulombic wave function of a colour-singlet $\tilde{g}\tilde{g}$ S-wave state evaluated at the origin (c.f. Refs. [47, 48]).

$$|\psi_{\tilde{g}}(0)|^2 \;=\; \frac{Z_g}{1 - \exp(-Z_g)} \tag{71}$$

with

$$Z_g \;=\; \frac{3\pi\alpha_S(p_C)}{\beta_{\tilde{g}}}, \tag{72}$$

where $\beta_{\tilde{g}} \;=\; \sqrt{1 - 4m_{\tilde{g}}^2/M^2}$ is the velocity of the $\tilde{g}$. It looks natural to choose the scale of α_S in (72) to be $p_C = \max\left\{(m_{\tilde{g}}(M - 2m_{\tilde{g}}))^{1/2}, (m_{\tilde{g}}\Delta M)^{1/2}\right\}$.

Since $Z_g \gtrsim 1$, QCD Coulombic effects drastically modify the $\tilde{g}\tilde{g}$ excitation curve, strongly enhancing the production rate at or near threshold. According to (70), for $Z_g^2 < 4\pi^2$ the threshold cross section rises with increasing $\beta_{\tilde{g}}$ approximately as $\beta_{\tilde{g}}^2$, rather than $\beta_{\tilde{g}}^3$ as one would expect from the Born result. Moreover, for $Z_g^2 \gg 4\pi^2$, the colour Coulombic exchanges in the final state completely compensate the kinematical $\beta_{\tilde{g}}^3$ threshold factor contained in the Born cross section [42, 45]

$$\beta_{\tilde{g}}^3 \, \frac{d\sigma_P(\tilde{g}\tilde{g}; M)}{d\sigma_P^{(0)}(\tilde{g}\tilde{g}; M)} \;\to\; \frac{27\pi}{4}\, \alpha_S^3(p_C) \;\simeq\; 0.14, \tag{73}$$

for $p_C \simeq 8$ GeV which corresponds to $\Delta M \simeq 1$ GeV. This is a dramatic effect relative to the lowest-order expectation. The (LSP) gluino-pair production process would lead to distinctive signatures in hadronic collisions, in particular to events with jets accompanied by missing p_T, see, for details, Ref. [43, 49].

Despite all the attractive features of the gluino-LSP scenario [43], it is possible that direct experimental studies at the Tevatron will close this window.

3.5.2 Gluino and squark production

A more plausible scenario is to search for massive unstable gluinos $\tilde{g}$ or squarks $\tilde{q}$, which will reveal themselves as multijet final states with missing energy and/or leptons[13]. As noted above the advantage of exclusive double-diffractive studies is that gluinos and squarks can be separated by their respective β^3 and β threshold behaviour. The Born subprocess cross sections are

$$\frac{d\hat{\sigma}^{\rm excl}}{dt}(gg^{PP} \to \tilde{g}\tilde{g}) = \frac{27}{2}\,\frac{1}{2}\,\frac{\pi\alpha_S^2}{6E_T^4}\,\frac{m_{\tilde{g}}^2}{M^2}\,\beta_{\tilde{g}}^2, \tag{74}$$

$$\frac{d\hat{\sigma}^{\rm incl}}{dt}(gg^{PP} \to \tilde{g}\tilde{g}) = \frac{27}{2}\,\frac{1}{2}\,\frac{\pi\alpha_S^2}{6E_T^2M^2}\left[\left(1-\frac{2E_T^2}{M^2}\right)\left(1-\frac{2m_{\tilde{g}}^2}{E_T^2}\right) + \frac{m_{\tilde{g}}^2}{E_T^2}\left(1+\beta_{\tilde{g}}^2\right)\right], \tag{75}$$

$$\frac{d\hat{\sigma}^{\rm excl}}{dt}(gg^{PP} \to \tilde{q}\bar{\tilde{q}}) = \frac{4\pi\alpha_S^2}{12M^4}\,\frac{m_{\tilde{q}}^4}{E_T^4}, \tag{76}$$

$$\frac{d\hat{\sigma}^{\rm incl}}{dt}(gg^{PP} \to \tilde{q}\bar{\tilde{q}}) = \frac{2\pi\alpha_S^2}{12M^4}\left(1 - \frac{2m_{\tilde{q}}^2}{E_T^2} + \frac{2m_{\tilde{q}}^4}{E_T^4}\right). \tag{77}$$

Note that (74) and (75) are the same as (50) and (52) for colour-singlet $gg \to q\bar{q}$, except for the colour-factor 27/2, and a factor 1/2 which reflects the Majorana nature of the two gluinos. The β^3 behaviour of exclusive gluino-pair production arises from β^2 of the last factor of (74) and β from the integration over t. The cross sections shown in (76) and (77) are written for one flavour and one type (L or R) of squark $\tilde{q}$.

Near threshold the formula have to be modified to account for sparticle widths and the QCD Coulomb interaction [41, 42]. Unfortunately the cross sections are very small near threshold. For example, if we take sparticle masses of 250 GeV and integrate from threshold (500 GeV) up to 625 GeV, then we find

$$\Delta\hat{\sigma}^{\rm excl}(\tilde{g}\tilde{g}) \simeq 6.5 \text{ pb}, \qquad \Delta\hat{\sigma}^{\rm excl}(\tilde{q}\bar{\tilde{q}}) \simeq 1.8 \text{ pb}. \tag{78}$$

For comparison the $t\bar{t}$ cross section, integrated from threshold up to 437 GeV, corresponding to the same value of $\beta = 0.6$, is

$$\Delta\hat{\sigma}^{\rm excl}(t\bar{t}) \simeq 2.2 \text{ pb}. \tag{79}$$

After multiplying by the double-diffractive luminosities of 2×10^{-5} for $\tilde{g}\tilde{g}$ and 4×10^{-5} for $t\bar{t}$ we have

$$\Delta\sigma(pp \to p + \tilde{g}\tilde{g} + p) \simeq 0.15 \text{ fb} \tag{80}$$

$$\Delta\sigma(pp \to p + \tilde{q}\bar{\tilde{q}} + p) \simeq 0.04 \text{ fb} \tag{81}$$

$$\Delta\sigma(pp \to p + t\bar{t} + p) \simeq 0.1 \text{ fb} \tag{82}$$

[13] At the moment we have no clear understanding which of these sparticles is the lightest, but the conventional belief is that the stop $\tilde{t}$ is the lightest squark.

for 'near' threshold production at the LHC. It is quite plausible that the masses of the light squark flavours are nearly degenerate, as are the masses of $\tilde{q}_L$ and $\tilde{q}_R$. This may allow a higher rate of $\tilde{q}\bar{\tilde{q}}$ events.

Another possibility to increase the yield of SUSY production is to consider the inclusive configuration of Fig. 1(b). Then the effective luminosity ($\sim 2 \times 10^{-3}$) is much larger. The corresponding subprocess cross sections, integrated from threshold (500 GeV) up to 625 GeV, are

$$\Delta\hat{\sigma}^{\rm incl}(\tilde{g}\tilde{g}) \simeq 24 \text{ pb}, \qquad \Delta\hat{\sigma}^{\rm incl}(\tilde{q}\bar{\tilde{q}}) \simeq 1 \text{ pb}, \tag{83}$$

leading to

$$\Delta\sigma(pp \to X + \tilde{g}\tilde{g} + Y) \simeq 50 \text{ fb}, \tag{84}$$

$$\Delta\sigma(pp \to X + \tilde{q}\bar{\tilde{q}} + Y) \simeq 2 \text{ fb}. \tag{85}$$

3.6 Soft Phenomena

Finally, we discuss the possibility to study soft strong interactions in diffractive events with two (or more) rapidity gaps (see, for example, [50, 51]). The (total) cross section of the Pomeron-Pomeron interaction is proportional to the square of the triple Pomeron coupling $g_{3I\!P}$. If we take the parameters from the analysis of Ref. [3] then we obtain the subprocess cross section

$$\hat{\sigma}_t(I\!P I\!P) \simeq 1.2 \text{ mb}. \tag{86}$$

When we multiply by the "soft $I\!P I\!P$" luminosity of Section 2.3, shown in Fig. 2, we predict a two rapidity gap cross section

$$\sigma_2 \sim 1 - 10 \ \mu\text{b}, \tag{87}$$

depending on the gap size. For the LHC it gives a very large event rate, which may be measured in a low luminosity (high β optics) run.

Such events offer an excellent opportunity to answer the many outstanding, interesting questions which remain from the intensive studies of soft physics of 25 or more years ago (see, for example, [51, 52]). A key problem is that the cross section of events containing n rapidity gaps is of the form

$$\sigma_n \sim (g_{3I\!P} \ln s)^{2n}/(2n)!, \tag{88}$$

which grows with energy. On summing, we have a cross section $\sigma \sim (s)^{g_{3I\!P}}$, which appears to violate unitarity. We must find a mechanism to suppress this huge cross section. We recall the scenarios which were considered long ago.

(i) To obtain a self consistent asymptotic theory it was proposed that the triple Pomeron coupling vanishes when the momentum transferred through the Pomeron goes to zero,

$$g_{3I\!P}(t) \to 0 \qquad \text{as} \qquad t \to 0. \tag{89}$$

The diffractive data do not confirm this proposal, although in the presence of strong $I\!P$-cuts it is still an open question. The study of double-Pomeron-exchange processes in low luminosity LHC runs, where the small t region becomes accessible, would clarify the situation (see [52] and references therein).

(ii) It was suggested that the soft survival probability $\hat{S}^2$ becomes much smaller for events with many gaps. The available CDF data [53], on double and single diffractive production, indicate otherwise, but again it should be checked at LHC energies.

(iii) It is more natural to expect $\hat{S}^2$ does not depend strongly on the number of gaps, but rather to propose that $\hat{S}^2$ decreases rapidly with increasing energy. In this scenario, rapidity gap events *only* occur in peripheral (large impact parameter) collisions where the opacity $\Omega(b)$ is still small. It follows that mean transverse momentum of the secondaries $\langle k_t \rangle$ created in the central $I\!P I\!P I\!P$ collisions of Fig. 1(c) will be smaller than $\langle k_t \rangle$ for the usual inelastic interaction at an equivalent energy, $\sqrt{s_{\rm inel}} = M$ [54]. This prediction could be checked at the LHC.

We emphasize that processes with 3 or more rapidity gaps have not yet been seen. It is clearly crucial to detect such events. To estimate $\sigma_3, \sigma_4, \ldots$, we assume factorization, and the same survival factor $\hat{S}^2$ for $\sigma_1, \sigma_2, \sigma_3, \ldots$. Then the probability to observe an additional rapidity gap will be

$$\omega_{\rm gap} \;=\; \left(\frac{\sigma^{DD}}{\sigma_{\rm inel} \hat{S}^2} \right), \tag{90}$$

where we cancel the factor $\hat{S}^2$ in the empirical double-diffractive cross section σ_{DD}, since the survival factor $\hat{S}^2$ is the same for all σ_n. Of course, we have to account for the phase space available for each gap. To make a phenomenological estimate, we start with the two-gap process of Fig. 1(c) and evaluate the probability to observe a third gap at the Pomeron-Pomeron energy $\sqrt{s_{I\!P I\!P}} = M$. For the LHC it corresponds to $\sqrt{s_{I\!P I\!P}} \sim 300$ GeV. Using the existing data in the ISR to Tevatron energy range, together with the $\hat{S}^2$ calculations of Ref. [3], we find

$$\omega_{\rm gap} \;\simeq\; 0.2 - 0.4 \tag{91}$$

and

$$\sigma_3 \;\simeq\; \omega_{\rm gap} \sigma_2 \;\sim\; 0.3 - 3 \;\mu{\rm b}. \tag{92}$$

Another possible soft phenomenon which is worth investigation is the "elastic" Pomeron-Pomeron scattering process

$$I\!P I\!P \;\to\; X^G Y^G, \tag{93}$$

where X^G and Y^G are glueball states. We call it elastic as the glueballs may lie on the Pomeron trajectory. That is there may exist a glueball dominance model of the Pomeron, in analogy to the vector meson dominance model of the photon.

4 Conclusions

In this paper we summarize, and extend, the results of our previous studies of double-diffractive processes with a rapidity gap on either side of a centrally produced heavy system. We have attempted to present the results in a unified, and user-friendly, form so that the expected cross sections at the Tevatron and the LHC can be readily estimated, simply by multiplying the appropriate luminosity of Section 2 with the relevant subprocess cross section $\hat{\sigma}$ of Section 3. We hope that it provides a useful framework to study double-diffractive phenomena, not only in their own right but also as a tool to probe physics beyond the Standard Model. Although many cross sections are predicted to be small, there are several interesting processes with viable signals. In particular, the exclusive double-diffractive production of an intermediate mass Higgs boson at the LHC, and the possibility of using the Tevatron and the LHC as a 'pure' gluon factory. For example, for the production of a Higgs boson of mass $M_H = 120$ GeV at the LHC we predict a cross section

$$\sigma(pp \to p + H + p) \;\simeq\; 3 \text{ fb}, \tag{94}$$

with a signal-to-QCD background ratio of

$$\frac{S(H \to b\bar{b})}{B(b\bar{b})} \;\gtrsim\; 15 \left(\frac{250 \text{ MeV}}{\Delta M}\right), \tag{95}$$

where ΔM is the experimental missing-mass resolution.

Acknowledgements

We thank Mike Albrow, Brian Cox, Gian Giudice, Dino Goulianos, Beate Heinemann, Aliosha Kaidalov, Risto Orava, Robi Peschanski, Krzysztof Piotrzkowski, Stuart Raby, Albert de Roeck, Andrei Shuvaev, Stefan Tapprogge and Georg Weiglein for interesting discussions. One of us (VAK) thanks the Leverhulme Trust for a Fellowship. This work was partially supported by the UK Particle Physics and Astronomy Research Council, by the Russian Fund for Fundamental Research (grants 01-02-17095 and 00-15-96610) and by the EU Framework TMR programme, contract FMRX-CT98-0194 (DG 12-MIHT).

References

[1] V.A. Khoze, A.D. Martin and M.G. Ryskin `hep-ph/0006005`, in *Proc. of 8th Int. Workshop on Deep Inelastic Scattering and QCD (DIS2000)*, Liverpool, eds. J. Gracey and T. Greenshaw (World Scientific, 2001), p.592.

[2] V.A. Khoze, A.D. Martin and M.G. Ryskin, Eur. Phys. J. **C19** (2001) 477, Erratum, ibid **C20** (2001) 599.

[3] V.A. Khoze, A.D. Martin and M.G. Ryskin, Eur. Phys. J. **C18** (2000) 167.

[4] A.B. Kaidalov, V.A. Khoze, A.D. Martin and M.G. Ryskin, Eur. Phys. J. **C21** (2001) 521.

[5] V.A. Khoze, A.D. Martin and M.G. Ryskin, Eur. Phys. J. **C14** (2000) 525.

[6] A. Levy, Phys. Lett. **B424** (1998) 191.

[7] A.D. Martin and M.G. Ryskin, Phys. Rev. **D64** (2001) 094017.

[8] A.G. Shuvaev, K.J. Golec-Biernat, A.D. Martin and M.G. Ryskin, Phys. Rev. **D60** (1999) 014015.

[9] A.D. Martin, R.G. Roberts, W.J. Stirling and R.S. Thorne, Eur. Phys. J. **C14** (2000) 133.

[10] A.D. Martin, M.G. Ryskin and V.A. Khoze, Phys. Rev. **D56** (1997) 5867.

[11] J.R. Forshaw and M.G. Ryskin, Z. Phys. **C68** (1995) 137.

[12] B.E. Cox, J.R. Forshaw and B. Heinemann, `hep-ph/0110173`.

[13] M. Boonekamp, R. Peschanski and C. Royon, `hep-ph/0107113`.

[14] F.E. Low, Phys. Rev. **D12** (1975) 163.

[15] S. Nussinov, Phys. Rev. Lett. **34** (1976) 1286.

[16] G. Ingelman and P.E. Schlein, Phys. Lett. **B152** (1985) 256.

[17] A. Donnachie and P.V. Landshoff, Phys. Lett. **B296** (1992) 227.

[18] H1 Collaboration: C. Adloff et al., Z. Phys. **C76** (1997) 613.

[19] M. Spira, A. Djouadi, D. Graudenz and P. Zerwas, Nucl. Phys. **B453** (1995) 17.

[20] Z. Künszt, S. Moretti and W.J. Stirling, Z. Phys. **C74** (1997) 479.

[21] J. Pumplin, Phys. Rev. **D47** (1993) 4820.

[22] Feng Yuan, Phys. Lett. **B510** (2001) 155.

[23] R. Barbieri, M. Gaffo, R. Gatto and E. Remiddi, Phys. Lett. **B95** (1980) 93, Nucl. Phys. **B192** (1981) 61.

[24] S. Kim, Nucl. Phys. **B** (Proc. Suppl.) **47** (1996) 437.

[25] E. Papageorgiu, Phys. Lett. **B352** (1995) 394.

[26] V.A. Khoze, A.D. Martin and M.G. Ryskin, `hep-ph/0103007`, in *Forward Physics and Luminosity Determination at the LHC*, Helsinki, Nov. 2000, eds. K. Huitu et al. (World Scientific, 2001), p.63.

[27] R.N. Cahn, S.D. Ellis, R. Kleiss and W.J. Stirling, Phys. Rev. **D35** (1987) 1626.

[28] N. Kauer, T. Plehn, D. Rainwater and D. Zeppenfeld, Phys. Lett. **B503** (2001) 113, and references therein.

[29] V.A. Khoze, A.D. Martin and M.G. Ryskin, Eur. Phys. J. **C21** (2001) 99.

[30] A. Berera and J.C. Collins, Nucl. Phys. **B474** (1996) 183.

[31] V.S. Fadin, V.A. Khoze and A.D. Martin, Phys. Rev. **D56** (1997) 484.

[32] A. Bialas and W. Szeremeta, Phys. Lett. **B296** (1992) 191;
A. Bialas and R. Janik, Z. Phys. **C62** (1994) 487.

[33] J. Pumplin, Phys. Rev. **D52** (1995) 1477.

[34] A.D. Martin, M.G. Ryskin and T. Teubner, Phys. Rev. **D62** (2000) 014022.

[35] CDF Collaboration: T. Affolder et al., Phys. Rev. Lett. **85** (2000) 4215.

[36] D.L. Borden et al., Phys. Rev. **D50** (1994) 4449;
M. Melles, W.J. Stirling and V.A. Khoze, Phys. Rev. **D61** (2000) 054015.

[37] A.I. Akhiezer, Physik. Z. Sowjetunion **11** (1937) 263;
R. Karplus and M. Neumann, Phys. Rev. **80** (1950) 380; *ibid* **83** (1957) 776;
B. De Tollis, Nuovo Cimento **32** (1967) 757; *ibid* **35** (1965) 1182;
Z. Bern et al., `hep-ph/0109079` and references therein.

[38] N. Arkani-Hamed, S. Dimopoulos and G. Dvali, Phys. Lett. **B429** (1998) 263;
I. Antoniadis, N. Arkani-Hamed, S. Dimopoulos and G. Dvali, Phys. Lett. **B436** (1998) 257.

[39] K. Cheung, Phys. Rev. **D61** (2000) 015005.

[40] H. Davoudiasl, Phys. Rev. **D60** (1999) 084022; Int. J. Mod. Phys. **A15** (2000) 2613.

[41] V.S. Fadin and V.A. Khoze, JETP Lett. **46** (1987) 525; Sov. J. Nucl. Phys. **48** (1988) 309.

[42] V.S. Fadin and V.A. Khoze, Sov. J. Nucl. Phys. **53** (1991) 692;
I.I. Bigi, F. Gabbiani and V.A. Khoze, Nucl. Phys. **B406** (1993) 3.

[43] A. Mafi and S. Raby, Phys. Rev. **D62** (2000) 035003, and refs. therein.

[44] T. Goldman and H. Haber, Physica **15D** (1985) 181.

[45] I.I. Bigi, V.S. Fadin and V.A. Khoze, Nucl. Phys. **B377** (1992) 461.

[46] K.A. Tumanov, Zh. Eksp. Teor. Fiz. (USSR), **25** (1953) 385;
A.I. Alekseev, Sov. Phys. JETP **7** (1958) 826.

[47] A. Sommerfeld, Atombau und Spektrallinien (Vieweg, Braunschweig, 1939), Vol. 2;
A.D. Sakharov, Zh. Eksp. Teor. Fiz. **18** (1948) 631.

[48] T.W. Appelquist and H.D. Politzer, Phys. Rev. Lett. **34** (1975) 43; Phys. Rev. **D12** (1976) 1404.

[49] H. Baer, K. Cheung and J.F. Gunion, Phys. Rev. **D59** (1999) 075002.

[50] Ya.I. Azimov, E.M. Levin, M.G. Ryskin and V.A. Khoze, Sov. J. Nucl. Phys. **21** (1975) 215.

[51] A.B. Kaidalov, Phys. Rep. **50** (1979) 157.

[52] Ya.I. Azimov, V.A. Khoze, E.M. Levin and M.G. Ryskin, Nucl. Phys. **B89** (1975) 508.

[53] For a recent review see K. Goulianos (for CDF Collaboration), `hep-ex/0109024`, and references therein.

[54] M.G. Ryskin, Sov. J. Nucl. Phys. **50** (1989) 289; Preprint LNPI-1419 (1988).